IEEE Photonics Journal
An IEEE Photonics Society Publication

Open Access

Sensitive and Specific Protein Sensing Using Single-Mode Tapered Fiber Immobilized With Biorecognition Molecules

Volume 7, Number 6, December 2015

Y. Mustapha Kamil, Member, IEEE
M. H. Abu Bakar, Member, IEEE
M. A. Mustapa
M. H. Yaacob, Member, IEEE
A. Syahir
M. A. Mahdi, Senior Member, IEEE

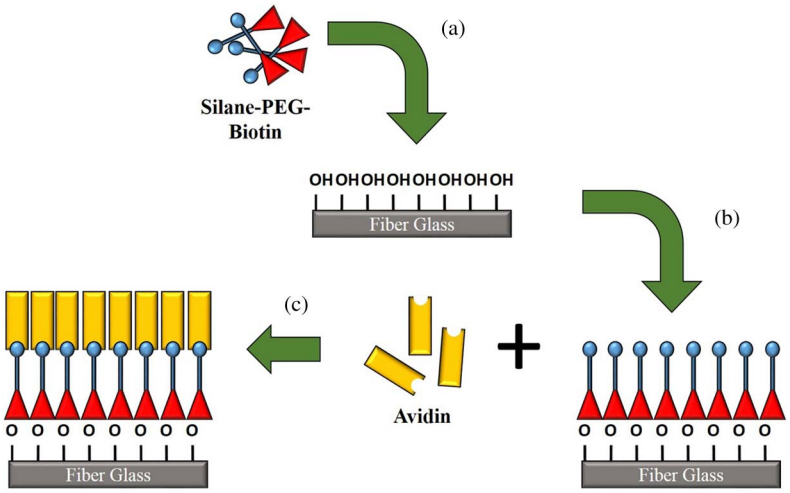

DOI: 10.1109/JPHOT.2015.2490486
1943-0655 © 2015 IEEE

IEEE photonics SOCIETY

IEEE

Sensitive and Specific Protein Sensing Using Single-Mode Tapered Fiber Immobilized With Biorecognition Molecules

Y. Mustapha Kamil,[1] *Member, IEEE*, M. H. Abu Bakar,[1] *Member, IEEE*, M. A. Mustapa,[1] M. H. Yaacob,[1] *Member, IEEE*, A. Syahir,[2] and M. A. Mahdi,[1] *Senior Member, IEEE*

[1]Research Centre of Excellence for Wireless and Photonic Networks, Faculty of Engineering, Universiti Putra Malaysia, 43400 Serdang, Malaysia
[2]Department of Biochemistry, Faculty of Biotechnology and Biomolecular Sciences, Universiti Putra Malaysia, 43400 Serdang, Malaysia

DOI: 10.1109/JPHOT.2015.2490486
1943-0655 © 2015 IEEE. Translations and content mining are permitted for academic research only. Personal use is also permitted, but republication/redistribution requires IEEE permission. See http://www.ieee.org/publications_standards/publications/rights/index.html for more information.

Manuscript received July 3, 2015; revised October 7, 2015; accepted October 9, 2015. Date of publication October 13, 2015; date of current version October 26, 2015. This work was supported by the Universiti Putra Malaysia's Graduate Research Fellowship, as well as the Ministry of Higher Education Malaysia's MyBrain scholarship and Fundamental Research Grant Scheme #FRGS/1/2014/STG08/UPM/01/29. Corresponding author: M. H. Abu Bakar (e-mail: mhab@ieee.org).

Abstract: We examine and demonstrate a biosensor using single-mode tapered fiber that has been immobilized with biorecognition molecules to sense targeted proteins. Interaction of evanescent waves with the external medium surrounding the tapered region produces an interferometric-patterned spectrum, which shifts correspondingly to any changes of refractive index (RI) in the external medium. The proposed setup managed to obtain an RI sensitivity and concentration sensitivity of 2526.8 nm/RIU and 20.368 nm/μM, respectively, which, to our knowledge, is highly sensitive when compared with previous studies. The dynamic performance, good specificity, and high sensitivity of the proposed method highlight an immensely beneficial choice for immunological diagnostics.

Index Terms: Tapered microfiber, refractive-index sensor, biosensors, biophotonics instrumentation.

1. Introduction

The prodigious use of fiber optic sensors has become a crucial factor in supporting the rapid evolution of the diagnostic field today. While conventional detection methods often depend on bulky instruments and heavy manual labor, fiber optics offer attractive alternatives that are more versatile, miniaturized, robust, affordable, immune to electromagnetic interferences and highly sensitive. With such credibility, they are known to be among the preferred choices in many sensing applications, including gene expression analysis, pharmaco-genetics, drug screening, forensics, and environmental monitoring [1], [2]. For the past few decades, the development of optical biosensors seems to show promising progress. Among them, tapered single-mode fibers have been known to be a favorite, especially in developing simple devices that are particularly sensitive to changes of its surrounding refractive index [3]–[6].

In general, the tapering process allows the excitation of higher order modes to be guided through the cladding, which now forms the new core along the tapered region. The evanescent waves generated along this region will interact with the surrounding external medium and produce measurable changes in the output transmission spectrum. Among related work incorporating the stated concept includes a single-mode tapered fiber as a refractive index sensor which was proposed to have ultra-high sensitivity when tested with various solutions in bulk [7]. Our research group had also done similar work to accentuate the exceptional sensitivity of the tapered fiber in sensing different concentrations of gelatin [8].

However, in the fields of environmental and biological diagnostics, where essential sensing of precise molecular determinants is desired, high sensitivity alone is not sufficient. Instead, specificity of the system should be greatly considered for such purposes. Each molecular determinant has a conformation or unique shape of its own, allowing them to selectively recognize and interact with molecules that mirror-image or complement them, like the key and lock configuration [9]. One way to enhance the specificity of the sensor system is to deploy the complementary concept as bio-recognition molecules so that the sensor will only sense the presence of the specific determinant of interest without the interference of other substances. The aforementioned experiments [7], [8], although exhibiting good sensitivity, were not designed to be sensitive towards a specific target and, thus, may detect changes caused by anything surrounding the sensing area.

The Biotin-Avidin system is a well-known bio-recognition complex in the world of molecular diagnostics. Their strong non-covalent protein-ligand interaction, with a high dissociation constant value of $K_D = 10^{-15}$ M [10], has made them very useful in applications concerning drug delivery [11], labeling [12], and detection [13]. By having one part, either biotin or Avidin, bound on the surface of the sensor, any biomolecules can be easily immobilized provided that they are labeled with the complement. A previous study showed promising selectivity of a surface plasmon resonance based biosensor in monitoring antigens using the biotin-Avidin system as a model [13]. Another study assessed the performance of a dielectric filled silicon acoustic sensor by verifying with biotin-Avidin (streptavidin) binding interactions [14]. In recent times, photonic crystal micro-cavity designs have shown impressive sensing performance but this method is plagued by issues in terms of light coupling, as well as complex fabrication process and long detection time [15].

An all-fiber platform offers seamless integration and direct biological interaction with simpler fabrication and operating methods. In this report, we demonstrate an optimized biosensor using a single-mode tapered fiber with immobilized silane-PEG-Biotin as bio-recognition molecules to sense the targeted protein, Avidin. The immobilization of specific bio-recognition molecules on the tapered surface is to improve and heighten the specificity of the biosensor. Aside from that, immobilization of the Biotin molecule is conducted by implementing the silanization method. Fabrication of tapered fibers is controlled accurately with a precise machine that has proven its reproducibility [16]. Findings from the proposed setup may contribute greatly to the development of highly sensitive bio-chemical sensing methods.

2. Sensing Principle

Propagation of light in an optical fiber is well explained by the principle of total internal reflection, where the differences of refractive index (RI) between the core and the cladding layers $(n_{core} > n_{clad})$ allow strong confinement of light within the core. However, when an optical fiber is tapered, the core/cladding interface is redefined in such a way that causes a portion of the fundamental core mode to be converted to higher-order cladding modes [17]. The schematic diagram of the tapered fiber is as illustrated in Fig. 1.

As the down-taper region excites these higher-order modes, they continuously propagate within the cladding of the tapered fiber which is now the new core, creating an evanescent field on the new core/external medium interface. The evanescent field is capable to interact with the

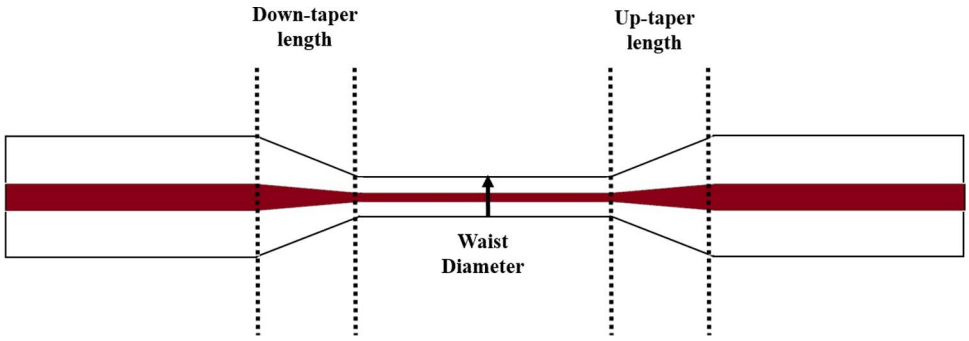

Fig. 1. Schematic diagram of a symmetrical tapered fiber.

surrounding environment and is highly sensitive depending on its penetration depth that decays exponentially [18]. The penetration depth can be mathematically expressed as [18]

$$d_p = \frac{\lambda}{2\pi\left(n_1^2 \sin^2\theta_{\text{int}} - n_{aq}^2\right)^{\frac{1}{2}}} \tag{1}$$

where λ is the wavelength of the incident light, n_1 and n_{aq} are the RI of the new core and the surrounding medium, and θ_{int} is the incident angle measured from the normal at the new core—external medium interface. Upon reaching the up-taper region, the fundamental and the high-order modes merge or couple back together into the fiber's original core, and because these modes are not in-phase with one another, the output spectrum will result in a Mach–Zehnder interferometric pattern. The intensity of the output is expressed as [8]

$$I = I_1 + I_2 + 2\sqrt{I_1 I_2}\cos(\Delta\Phi) \tag{2}$$

where I is the output intensity; I_1 and I_2 are the intensities of the fundamental core mode and the high-order modes, respectively; and $\Delta\Phi$ is the phase shift between the two modes, which is calculated using [8]

$$\Delta\Phi = \left[\frac{2\pi(\Delta n_{\text{eff}})L_w}{\lambda}\right] \tag{3}$$

where Δn_{eff} is the difference between the effective refractive index of the core and the effective refractive index of the external surrounding $(n_c^{\text{eff}} - n_{\text{ext}}^{\text{eff}})$, and L_w is the waist length. The fringe spacing between two interference patterns is given by [8]

$$\Lambda = \frac{\lambda^2}{(\Delta n_{\text{eff}})L_w}. \tag{4}$$

These equations mathematically support the idea that any manipulation of RI at the external surrounding or the cladding would affect the phase shift, fringe shift, as well as the resulting intensity of the output. Hence, when a sample of interest or a targeted analyte is introduced to the system, the occurrence of change in refractive index will be shown as the shifting of interference pattern between the spectra, as well as the difference in output intensity.

3. Methodology

3.1. Fabrication of Tapered Fibers

The light transmission within a tapered fiber is affected greatly by the physical dimensions of the tapered region. In this work, tapers were fabricated using Vytran's GPX-3400 Optical Glass Processing Workstation. The machine is capable of performing precise fusion splicing and

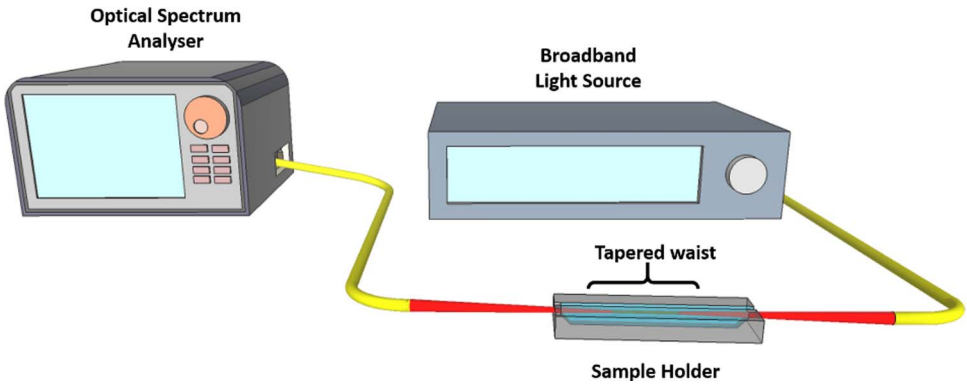

Fig. 2. Experimental setup for the performance measurement of the proposed tapered fiber sensor.

tapering with its filament furnace assembly and precision stages. Its real-time control system allows manipulation of dimensions, uniformity and reproducibility of the fabricated taper as the pulling speed and heat were kept at a constant value of 1 mm/s and 42 W, respectively. Using a standard step index single-mode fiber (Lucent All-Wave Fiber), a section was tapered down from the initial cladding diameter of 125 μm to 12.3 μm with symmetric up and down taper transition lengths of 5 mm, respectively. As for the tapered fiber's waist length, although an ultra-short waist length has been reported to achieve great sensitivity for bulk solution sensing [7], such a length would not provide enough surface area for the ligand-target protein interaction. Thus, the proposed work opted for a longer length; 15 mm, for all fabricated tapered fibers in the experiment. Dimensions were measured under the machine's microscope for confirmation.

Both ends were later connected to single mode pigtails with the input end fixed to a broadband light source from 1520 nm to 1620 nm (Amonics ALS 18-B-FA) and the output end to an optical spectrum analyzer (AQ6331 Yokogawa), as shown in Fig. 2.

3.2. Characterization of Tapered Fiber

Optical characteristics of the tapered fiber with the chosen taper profile were first obtained by testing its sensitivity with salt (NaCl) solution at different concentrations. The tapered region was secured within the groove of a customized sensing platform that was made to facilitate the immersion of the region to different solutions. Concentrations of NaCl used for the manipulation of RI were 0.1 M, 0.2 M, 0.3 M, 0.4 M, 0.5 M, and 0.6 M, which were prepared following the dilution method that satisfied the molarity equation. Prior to the sensitivity testing, RI readings for each concentration were taken using a digital pocket refractometer (ATAGO), which yielded RI readings in the range of 1.3332 to 1.3420. A steady transmission was obtained immediately after the immersion of the solutions. Readings were taken, and spectral output responses at each concentration were compared.

3.3. Immobilization of Biotinylated Silane Molecules

3.3.1. Surface Modification of Tapered Fibers With Hydroxyl Groups

Following characterization, the surface of the fabricated tapered fibers was modified by treating them with concentrated sodium hydroxide (NaOH) for 1 hour to enhance the attachment of hydroxyl groups (-OH) onto the tapered surface [19]. The hydroxyl groups are important to allow the covalent attachment of silane-PEG-Biotin compound onto the tapered fiber. Although method referred suggested 30 minutes of incubation time, we have found through initial trials that 45 minutes to 1 hour was required to reach a steady transmission state. Hence, 1 hour incubation time was implemented. Following the step, tapered fibers were rinsed with distilled water to remove the residual solution and then dried.

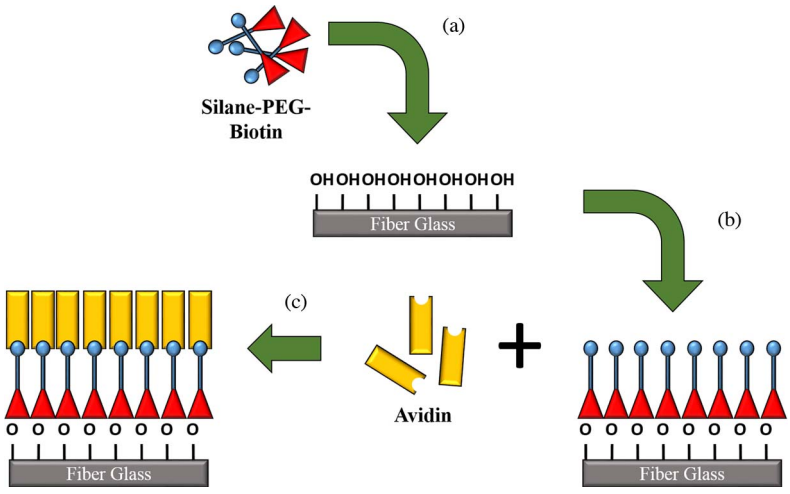

Fig. 3. Schematic figure to describe the (a) surface preparation, (b) functionalization, and (c) detection process.

3.3.2. Functionalization of Tapered Fibers With Silane-PEG-Biotin

Pre-treated tapered fibers were then incubated for 30 minutes with 0.1 M silane-PEG-biotin $(\text{RI} = 1.3508)$ in a mixture of ethanol/water (w/w, 95%/5%) following the methods used in [20], [21]. This allows the silane to react with the activated silica surface and immobilize on to it. Fibers were then rinsed with distilled water after functionalization to remove any unbound molecules and left to dry.

3.4. Detection of Avidin Binding Onto the Tapered Fiber

Once functionalized, the tapered fibers were introduced to increasing concentrations of Avidin that has been diluted in phosphate buffer solution (PBS) with a pH value of 7.4. Concentrations obtained were 0.2 μM, 0.4 μM, 0.6 μM, 0.8 μM, and 1.0 μM. The same PBS without Avidin was also tested as a negative reference. Incubation time with Avidin solutions is 15 minutes. Prior to this step, RI readings for each concentration were measured, which corresponded to an RI range between 1.3330–1.3376. The tapers were rinsed with distilled water after soaking in each concentration of Avidin to eliminate any residual molecules and were then dried. The rinse and dry step at the end of each stage is very important to ensure that any shifting of peaks in the output spectrum can be attributed solely to molecular immobilization or detachment on the tapered fiber. Readings were taken after each stage; modification, functionalization, and detection of Avidin (see Fig. 3), and spectral output trends were then analyzed. The whole experiment was conducted under room temperature of 25 °C that is monitored by a digital thermometer and all biological samples were kept in a 4 °C fridge with minimal thawing. To further assess the consistency and precision of the instrument, multiple sets of the same experiment were conducted using tapered fibers that have undergone the exact same fabrication method under identical conditions. Fabricated sensors were stored in a freezer at –20 °C.

4. Results

4.1. Characterization of Tapered Fiber

As depicted in Fig. 4(a), a red shift can be observed when the dip of the spectral responses were compared as the concentration of NaCl increases. This is due to the fact that the increase in concentration promotes an increase in RI as well. In accordance to Eq. (4), the increase of RI reduces the Δn_{eff} value, resulting in a larger fringe gap and red shifts. The trend line in Fig. 4(b) suggests good congruity between the two parameters with a correlation coefficient value of

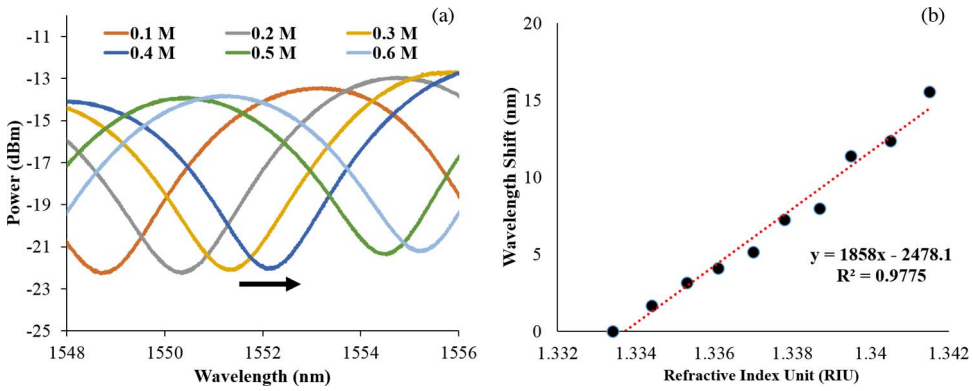

Fig. 4. (a) Spectral response of tapered fiber when immerse in different concentrations of NaCl and (b) a linear trend line depicting the relationship between wavelength shift and refractive index change.

$R^2 = 0.9775$. The sensitivity achieved is 1858.0 nm/RIU, which is considerably higher compared to previous studies [3], [8], [22] and comparable to [7] within the same range of RI.

4.2. Surface Modification and Functionalization of Tapered Fiber

Although the sensitivity for the proposed setup is attractively reliable with bulk liquid (also reported in [8]), it may behave differently for systems that heavily depend on specific binding of recognition molecules. One explanation to this is the non-homogeneous distribution of the targeted molecule attachment on the tapered region. Moreover, bulk solution cannot be attached specifically to a recognition molecule; hence, to justify the performance of the proposed transducer for such conditions, we functionalized the surface with silane-PEG-Biotin to determine its response to different concentrations of Avidin.

Among the best ways to promote conjugation between bio-active molecules with silica glass surfaces like a tapered optical fiber is with the use of silane coupling agents [23]. The silane agent on silane-PEG-Biotin molecule has three alkoxy functional groups and an organic group (-NH) that is readily attached to PEG-Biotin. Conjugation happens when the alkoxy group hydrolyses with silanols created on the surface of the tapered fiber, after being treated with NaOH, to form strong siloxane bonds. The bonding on the surface of the tapered fiber will cause an increase of RI that will result in a red shift of the spectra peaks.

This phenomenon can be observed in Fig. 5(a) and (b), which show the spectral responses of the tapered fiber after the surface modification process with NaOH and the functionalization process with silane-PEG-Biotin. The peak response after tapered fiber was immersed with NaOH shifts 3.77 nm to the right from the adjacent peak response before the treatment. Same observation was made after functionalization with silane-PEG-Biotin as the peak response shifted further to the right by 1.33 nm. The red shift observations indicate successful surface preparation and functionalization of silane-PEG-biotin onto the tapered region. Another trait to observe from the graph is the extinction ratio (ER), which is the difference between the highest and the lowest point of the spectrum. Fig. 5(a) show a 3.86 dB decrease in ER from 9.85 dB to 5.99 dB after the tapered fiber was immersed in NaOH. Further decrement was observed after the immobilization of Biotin. We suggest that this is due to the property change on the surface of the tapered fiber, causing the excited cladding modes to shift its phase further from its initial phase producing less efficient interferences when coupled back with the fundamental mode [24]. This observation validates the success of the surface preparation and functionalization procedures as well.

4.3. Specificity of Tapered Fiber When Tested With Avidin and PBS

After functionalization was achieved, the tapered fiber was introduced with Avidin, as well as Phosphate buffer solution (PBS), as a negative control to demonstrate the system's specificity.

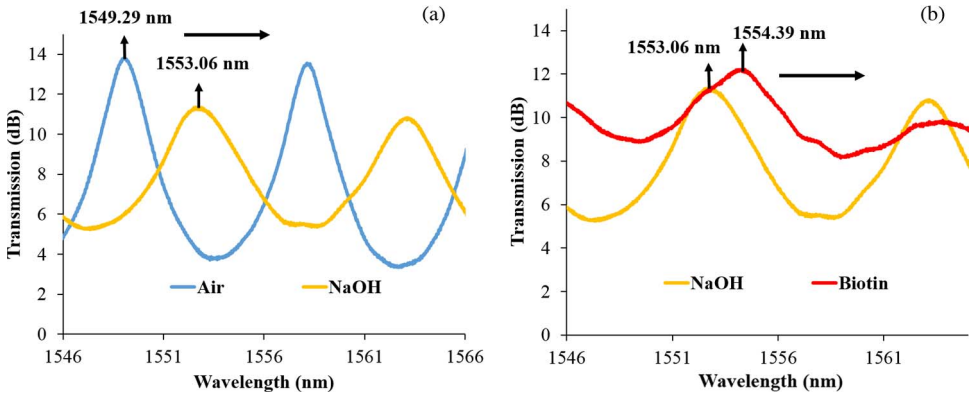

Fig. 5. (a) Transmission response of tapered fiber before and after the surface preparation process with NaOH and (b) transmission response of tapered fiber before and after the surface functionalization process with silane-PEG-Biotin.

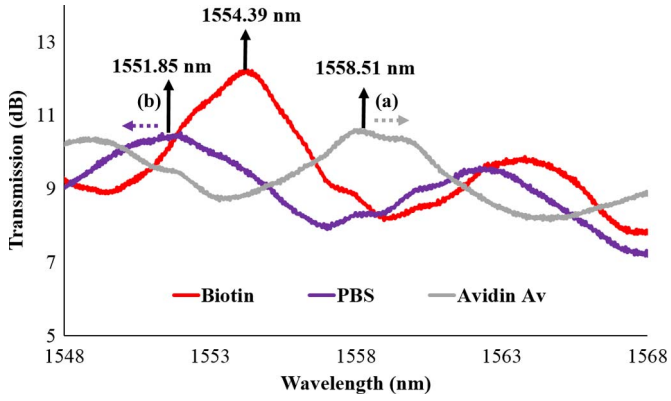

Fig. 6. Comparison of spectra responses when tapered fiber was introduced to silane-PEG-Biotin, PBS, and Avidin, where arrow (a) shows the red shift when Avidin was introduced and (b) the blue shift when PBS was introduced.

Should the sensor neglect the surface modification step and the specificity trait like [7], [8], spectra peaks should show Avidin at the lowest wavelength, followed by Biotin, and PBS with respect to the effects of their RI where Avidin at 0.2 nM corresponded to an RI value of 1.3544. However, Fig. 6 depicts the PBS spectrum having shifted 2.54 nm to the left from the peak of the Biotin spectrum, which suggests no binding occurred in the tapered region. On the other hand, the 4.12 nm shift to the right after the introduction of Avidin supports the successful capture of targeted Avidin molecules to the Biotin end of the silane-PEG-Biotin compound. The decreased ER obtained when Avidin was introduced strengthens the finding as the peak response of PBS has a higher ER compared to the rest.

4.4. Sensitivity of Tapered Fiber With Different Concentrations of Avidin

To analyze the sensitivity of the system, the tapered fiber was introduced to Avidin at different concentrations ranging from 0.2 μM to 1 μM. Fig. 7(a) shows a coherent linear trend line between the wavelength shifts corresponding to the changes of RI with a coefficient correlation value of $R^2 = 0.9533$. Again, a red shift observation is also present here as the concentration and RI increment promotes the shifting of antinodes to the bigger wavelength region. This suggests successful attachment of Avidin with the functionalized ligand silane-PEG-Biotin on the tapered area. The sensor recorded detection limit of 0.2 μM with RI and concentration sensitivity

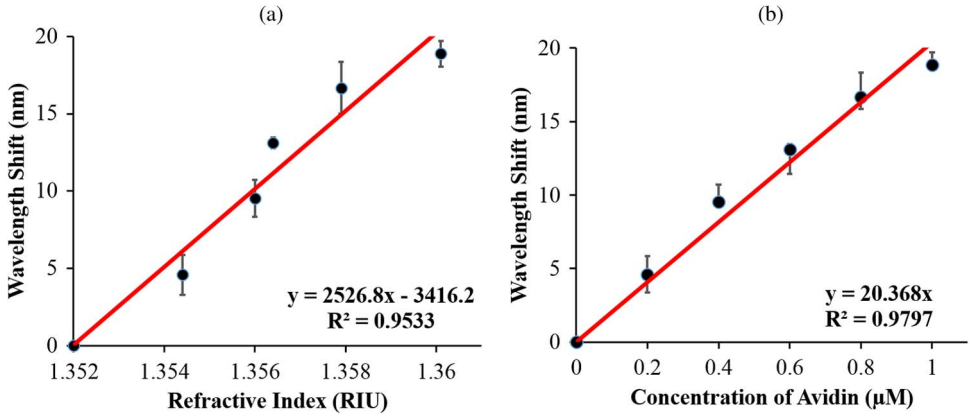

Fig. 7. (a) Linear trend exhibiting the relationship between wavelength shift, its corresponding refractive index change, and (b) wavelength shift and its corresponding concentration change when immersed in different concentrations of Avidin.

of 2526.8 nm/RIU and 20.368 nm/μM respectively, which is comparable or even better than recent reports on protein sensors [8], [25]–[28]. We postulate the occurrence was as such due to the promotion of specific binding on the tapered region that resulted in a more concentrated attachment of targeted molecules on the tapered surface when compared with the floating molecules in bulk solution. Thus, a smaller Δn_{eff} and a larger fringe gap were obtained which gave us the larger sensitivity value [29]. Fig. 7(b) depicts a trend line to describe the proportional relationship between the wavelength shifts produced and concentration change with $R^2 = 0.9797$. Error bars in both Fig. 7(a) and (b) represent standard deviation (SD±) of experimental triplicates. Low average SD± value of 0.51 denotes minimal variation within the system, which further favors the reproducibility of the sensor.

5. Conclusion

In conclusion, we have investigated the performance of a highly sensitive tapered fiber transducer and its response to specific molecular attachment between silane-PEG-biotin and Avidin. The proposed taper profile managed an RI and concentration sensitivity values of 2526.8 nm/RIU and 20.368 nm/μM, respectively. The successful integration of our setup with bio-recognition molecules has greatly enhanced its specificity by providing precise selectivity towards targeted substrate of interest. Good reproducibility has been portrayed as well with a low SD± value of 0.51. Due to irreversible binding constrictions, the proposed setup will be suitable for disposable test procedures, which is, in fact, a more preferable approach in light of hygiene issue. Today, bio-recognition molecules and complexes like Biotin and Avidin can be engineered to complement many hormone and antigenic proteins for the detection of various diseases and chemical compounds. With this advantage, along with the qualities of being highly sensitive, specific, reliable and cost effective, the proposed study may contribute greatly in the world of both environmental and medical diagnostics.

References

[1] J.-D. Kim and Y.-G. Lee, "Trapping of a single DNA molecule using nanoplasmonic structures for biosensor applications," *Biomed. Opt. Exp.*, vol. 5, no. 8, pp. 2471–2480, Aug. 2014.
[2] M. E. Bosch, A. Jesús, R. Sánchez, F. S. Rojas, and C. B. Ojeda, "Recent development in optical fiber biosensors," *Sensors*, vol. 7, no. 6, pp. 797–859, Jun. 2007.
[3] P. Wang *et al.*, "High-sensitivity, evanescent field refractometric sensor based on a tapered, multimode fiber interference," *Opt. Lett.*, vol. 36, no. 12, pp. 2233–2235, Jun. 2011.
[4] Y. Lin, Y. Zou, and R. G. Lindquist, "A reflection-based localized surface plasmon resonance fiber-optic probe for biochemical sensing," *Biomed. Opt. Exp.*, vol. 2, no. 3, pp. 478–484, Mar. 2011.

[5] J. Yang *et al.*, "Highly sensitive refractive index optical fiber sensors fabricated by a femtosecond laser," *IEEE Photon. J.*, vol. 3, no. 6, pp. 1189–1197, Dec. 2011.
[6] Y. Ran, L. Jin, L.-P. Sun, J. Li, and B.-O. Guan, "Temperature-compensated refractive-index sensing using a single Bragg grating in an abrupt fiber taper," *IEEE Photon. J.*, vol. 5, no. 2, Apr. 2013, Art. ID. 7100208.
[7] W. Bin *et al.*, "Ultra-high sensitivity refractive index sensor based on optical microfiber," *Photon. Technol. Lett.*, vol. 24, no. 20, pp. 1872–1874, Oct. 2012.
[8] T. K. Yadav, R. Narayanaswamy, M. H. Abu Bakar, Y. M. Kamil, and M. A. Mahdi, "Single mode tapered fiber-optic interferometer based refractive index sensor and its application to protein sensing," *Opt. Exp.*, vol. 22, no. 19, pp. 22802–22807, Sep. 2014.
[9] L. J. Kleinsmith, *Biological Specificity*. New York, NY, USA: McGraw-Hill, 2012.
[10] V. J. O'Sullivan *et al.*, "Development of a tetrameric streptavidin mutein with reversible biotin binding capability: Engineering a mobile loop as an exit door for biotin," *PLoS ONE*, vol. 7, no. 4, Apr. 2012, Art. ID. e35203.
[11] M.-H. Chen *et al.*, "A versatile drug delivery system using streptavidin-tagged pegylated liposomes and biotinylated biomaterials," *Int. J. Pharmaceutics*, vol. 454, no. 1, pp. 478–485, Sep. 2013.
[12] S. Goto, R. Morigaki, S. Okita, S. Nagahiro, and R. Kaji, "Development of a highly sensitive immunohistochemical method to detect neurochemical molecules in formalin-fixed and paraffin-embedded tissues from autopsied human brains," *Front. Neuroanat.*, vol. 9, pp. 22, Mar. 2015.
[13] Y. Mu *et al.*, "An optical biosensor for monitoring antigen recognition based on surface plasmon resonance using avidin-biotin system," *Sensors*, vol. 1, no. 3, pp. 91–101, Aug. 2001.
[14] A. Heidari *et al.*, "Biotin-streptavidin binding interactions of dielectric filled silicon bulk acoustic resonators for smart label-free biochemical sensor applications," *Sensors (Basel)*, vol. 14, no. 3, pp. 4585–4598, Mar. 2014.
[15] M. Scullion, M. Fischer, and T. Krauss, "Fibre coupled photonic crystal cavity arrays on transparent substrates for spatially resolved sensing," *Photonics*, vol. 1, no. 4, pp. 412–420, Nov. 2014.
[16] T. Guo, L. Shao, H. Tam, P. A. Krug, and J. Albert, "Tilted fiber grating accelerometer incorporating an abrupt biconical taper for cladding to core recoupling," *Opt. Exp.*, vol. 17, no. 23, pp. 20651–20660, Nov. 2009.
[17] P. Lu *et al.*, "Tapered-fiber-based refractive index sensor at an air/solution interface," *Appl. Opt.*, vol. 51, no. 30, pp. 7368–7373, Oct. 2012.
[18] M. Ahmad and L. L. Hench, "Effect of taper geometries and launch angle on evanescent wave penetration depth in optical fibers," *Biosens. Bioelectron.*, vol. 20, no. 7, pp. 1312–1319, Jan. 2005.
[19] W. L. W. Hau, D. W. Trau, N. J. Sucher, M. Wong, and Y. Zohar, "Surface-chemistry technology for microfluidics," *J. Micromech. Microeng.*, vol. 13, no. 2, pp. 272–278, Mar. 2003.
[20] A. Syahir, H. Mihara, and K. Kajikawa, "A new optical label-free biosensing platform based on a metal-insulator-metal structure," *Langmuir, ACS J. Surf. Colloids*, vol. 26, no. 8, pp. 6053–6057, Apr. 2010.
[21] Nanocs, New York, NY, USA, *Data Sheet: Silane PEG Biotin*, 2015.
[22] G. Yin, S. Lou, and H. Zou, "Refractive index sensor with asymmetrical fiber Mach–Zehnder interferometer based on concatenating single-mode abrupt taper and core-offset section," *Opt. Laser Technol.*, vol. 45, pp. 294–300, Feb. 2013.
[23] C. M. Modgi, A. M. Ajay, and V. Chitre, "Surface conditioning treatments for improving adhesion of fiber posts," *J. Orofacial Res.*, vol. 2, no. 1, pp. 37–41, Mar. 2012.
[24] G. Cheng, J. Wang, Z. Feng, and N. Chen, "Simultaneous twist angle and direction sensing using abrupt-tapered fiber Mach–Zehnder interferometers," in *Proc. 6th Int. Conf. Sens. Technol.*, 2012, pp. 460–463.
[25] D. Yang *et al.*, "High sensitivity and high Q-factor nanoslotted parallel quadrabeam photonic crystal cavity for real-time and label-free sensing," *Appl. Phys. Lett.*, vol. 105, no. 6, Aug. 2014, Art. ID. 063118.
[26] L. Bo *et al.*, "Microfiber coupler based label-free immunosensor," *Opt. Exp.*, vol. 22, no. 7, pp. 8150–8155, Apr. 2014.
[27] H. Oyama, K. Takahashi, N. Misawa, K. Okumura, and M. Ishida, "A MEMS based Fabry–Pérot protein sensor with reference sensor," in *Proc. 14th Int. Meet. Chem. Sens.*, 2012, pp. 352–355.
[28] C. Caucheteur, V. Voisin, and J. Albert, "Polarized spectral combs probe optical fiber surface plasmons," *Opt. Exp.*, vol. 21, no. 3, pp. 3055–3066, 2013.
[29] A. Leung, P. M. Shankar, and R. Mutharasan, "Model protein detection using antibody-immobilized Tapered Fiber Optic Biosensors (TFOBS) in a flow cell at 1310 nm and 1550 nm," *Sens. Actuat. B, Chem.*, vol. 129, no. 2, pp. 716–725, Feb. 2008.